

Research Repository UCD

Title	Rate of Entropy Production as a Physical Selection Principle for Mode-Mode Transitions in Non-Equilibrium Systems: With an Application to a Non-Algorithmic Dynamic Message Buffer
Authors(s)	Frank, Till D.
Publication date	2011-06
Publication information	Frank, Till D. "Rate of Entropy Production as a Physical Selection Principle for Mode-Mode Transitions in Non-Equilibrium Systems: With an Application to a Non-Algorithmic Dynamic Message Buffer." EuroJournals, June 2011.
Publisher	EuroJournals
Item record/more information	http://hdl.handle.net/10197/5036

Downloaded 2026-11-12 12:01:31

The UCD community has made this article openly available. Please share how this access benefits you. Your story matters! (@ucd_oa)



© Some rights reserved. For more information

European Journal of Scientific Research
ISSN 1450-216X Vol.54 No.1 (2011), pp.59-58
© EuroJournals Publishing, Inc. 2011
http://www.eurojournals.com/ejsr.htm

Rate of Entropy Production as a Physical Selection Principle for Mode-Mode Transitions in Non-Equilibrium Systems: With an Application to a Non-Algorithmic Dynamic Message Buffer

T. D. Frank
Center for the Ecological Study of Perception and Action, Department of Psychology
University of Connecticut, 406 Babbidge Road, CT, USA
E-mail: till.frank@uconn.edu
Tel: +1-860-4863906; Fax: +1-860-4862760

Abstract

We examine a generic set of amplitude equations proposed earlier by Haken that describes the emergence and bifurcations of modes and spatio-temporal patterns of self-organizing non-equilibrium systems. We relate feedback parameters occurring in the amplitude equations to pumping processes associated with entropy production. In doing so, we show that the rate of entropy production determines which mode-mode transitions are allowed and which not. Roughly speaking, transitions occur from modes of low rate of entropy production towards modes of high rate of entropy production (selection principle). In line with the recent efforts in the field of physical intelligence, we outline how physical, non-algorithmic, self-organizing systems satisfying Haken's amplitude equations may be used to design a dynamic input-output message buffer. The functioning of such a dynamic buffer again follows the aforementioned selection principle: the buffer switches between input and output modes in order to select modes with relatively high rates of entropy production. Moreover, only mode-mode transitions are allowed that increase the rate of entropy production of the active mode.

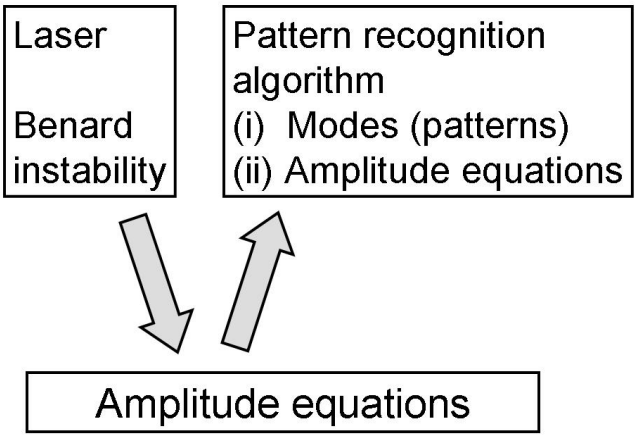
Keywords: Amplitude equations, rate of entropy production, selection principle, non-equilibrium systems, physical intelligence

1. Introduction

Haken observed that multistable pattern formation systems that have been studied extensively in physics can be used to solve problems of artificial intelligence [1, 2]. His constructive proof is sketched in Figure 1. On the one hand, for some benchmark examples of non-equilibrium self-organizing systems (lasers, convection cells, etc) amplitude equations have been derived that assume a certain mathematical structure [1-4]. On the other hand, inspired by this formal structure, Haken suggested a pattern recognition algorithm involving modes in form of to be recognized patterns and amplitude equations that determined the emergence of these modes. As a result, on the formal level of amplitude equations physical non-algorithmic systems satisfy the same kind of amplitude equations as algorithms implemented on computers that solve pattern recognition problems. Haken's argument found further support by a numerical study on the Swift-Hohenberg model for Benard instability in which it was

demonstrated that to a certain extent convection instabilities solve pattern recognition problems [3]. Haken's amplitude equations and generalized versions have found a variety of applications [5-16].

Figure 1: Physical non-algorithmic systems (lasers, fluid layers, etc) solving problems of artificial intelligence (pattern recognition).



While a large amount of research has been carried out in the field of artificial intelligence, the development of physical non-algorithmic systems that can deal with similar problems as their algorithmic counterparts of AI is still in its infancy. We may refer to such systems as smart physical systems – for the time being. Smart physical systems hold the promise to overcome limitations of artificial intelligence systems which is the reason why recent research efforts have been devoted to explore the development of physical systems exhibiting some kind of intelligence.

From a different perspective Swenson and Turvey [17] approached a similar problem: the nature of human intelligent behavior as reflected in the interplay between perception and performance (action). They argued that human intelligent motor-behavior (involving the interplay between perceptual processing and motor actions) must be based on physical selection principles and in particular thermodynamic principles of non-equilibrium systems. Taking the these two perspectives (Haken's perspective and the work by Swenson and Turvey) together, we arrive at the scheme illustrated in Table 1 that calls for exploring the link between intelligent behavior, physics and non-equilibrium thermodynamics.

Table 1: Two approaches calling for an understanding of human and artificial intelligence from physical first principles

Haken (Ref [1,2])	Physical self-organizing multistable systems	►	Intelligent devices
Swenson and Turvey (Ref [17])	Physical selection principlesNon-equilibrium thermodynamics	◄	Human intelligent behavior reflected in perception-action cycles

In Sec. 2 we will study in more detail the amplitude equations proposed by Haken. We will show how to take pumping processes into account that are relevant for the amplitude dynamics. In doing so, we will make contact with entropy production processes of various kind and will be able to show that the rate of entropy production governs transitions between mutually exclusive modes or spatio-temporal patterns. In sum, we will give explicit expressions to the ideas summarized in Table 1. Finally, in Sec. 3 we will apply our results to a simple version of a dynamic message buffer.

2. Bifurcations in Haken's Amplitude Equations and Thermodynamic Selection Principle via Rate of Entropy Production

2.1. Review: Amplitude Equations with Inhomogeneous Activation Parameter Spectrum

We consider a physical or chemical self-organizing system that exhibits a number of M modes or spatio-temporal patterns. For example a fluid layer in Benard instability may exhibit under certain conditions an infinite number of roll patterns that all are stable but differ in orientation [3]. Vertical cavity surface emitting laser devices can exhibit laser modes with two different polarizations [18,19]. Binary mixtures heated from below exhibit different types of traveling wave patterns [20]. Dissipative gas discharge systems exhibit dissipative solitons that can have an infinitely large number of modes of self-propagation [21-24]. Chemical systems (in particular bio-chemical systems involving enzyme reactions) exhibit on-off modes (bistability) where only one of two chemicals is present [25]. We focus next on systems that exhibit amplitude equations that have the following generic structure [1,2]

$$\frac{d}{dt}\xi_k = \lambda_k\ \xi_k - B\xi_k \sum_{m=1,m\neq k}^{M}\xi_m^2 - C\xi_k\sum_{m=1}^{M}\xi_m^2 \tag{1}$$

Here, $\xi_k(t)$ is the time-dependent amplitude of the kth mode and t is time. The parameters B and C are positive: $B,C>0$. The parameter λ_k is the activation parameter of the kth amplitude or mode and assumes positive or negative real values. When $\lambda_k>0$ then the magnitude of λ_k tells us how fast the amplitude would increase exponentially due to the linear term (i.e. when the impact of nonlinear terms would be neglected). As such the amplitudes ξ_k may assume negative values. For our purposes, we consider only initial conditions $\xi_k(0)>0$. In this case, the amplitudes remain semi-positive definite for all times. Consequently, we will disregard negative solutions in what follows. The amplitude equations (1) are known to represent a winners-takes-all model [2,15]. More precisely, the only stable stationary solutions of (1) are given by $\xi_h>0$ for one specific index h and $\xi_q=0$ for all other indices $q\neq h$. This result holds if there is at least one activation parameter λ_k larger than zero. If all activation parameters are negative then the only stationary fixed point is the origin. This fixed point is stable. In what follows, we will assume that there is at least one positive activation parameter and consequently can focus our considerations entirely on "winner-takes-all" fixed points. Let us re-write the amplitude equations (1) in rescaled amplitude variables. First, we re-arrange Eq. (1) like

$$\frac{d}{dt}\xi_k = \lambda_k\ \xi_k - (B+C)\xi_k \sum_{m=1,m\neq k}^{M}\xi_m^2 - C\xi_k^3 \tag{2}$$

Then, we substitute

$$\xi_k^* = \sqrt{C}\ \xi_k \tag{3}$$

into Eq. (2), which yields

$$\frac{d}{dt}\xi_k^* = \lambda_k\ \xi_k^* - \left(1+\frac{B}{C}\right)\xi_k^* \sum_{m=1,m\neq k}^{M}(\xi_m^*)^2 - (\xi_k^*)^3 \tag{4}$$

We drop the star and introduce the parameter

$$g = 1+\frac{B}{C} > 1 \tag{5}$$

such that Eq. (4) becomes

$$\frac{d}{dt}\xi_k = \lambda_k\ \xi_k - g\xi_k \sum_{m=1,m\neq k}^{M}\xi_m^2 - \xi_k^3 \tag{6}$$

Let us briefly review the stability analysis for Eq. (6) as derived in Ref [2,15]. For our purposes it is sufficient to assume that all activation parameters are positive: $\lambda_k>0$ for all k. Then, there are winner-takes-all fixed points and fixed points of other kind. Fixed points of the latter type are unstable. The winner-takes-all fixed points can be divided into stable and unstable ones. Let

$$\xi_h = \sqrt{\lambda_h} > 0 \quad , \quad \xi_q = 0 \; \forall \; q \neq h \tag{7}$$

denote the winner-takes-all fixed point of mode h (where h=1,…,M). Let λ_{max} denote the maximal activation parameter. Then the fixed point of mode h is stable if

$$\lambda_h > \frac{\lambda_{\max}}{g} \tag{8}$$

and unstable if

$$\lambda_h < \frac{\lambda_{\max}}{g} \tag{9}$$

As a result, the amplitude equations (6) exhibit a stability band defined by the interval (λ_{max}/g, λ_{max}]. All modes h that have activation parameters λ_h that belong to that stability band are stable modes. This also implies that the amplitude dynamics exhibits multistability for an appropriate choice of activation parameters [2,15].

2.2. Activation Parameters and Pumping

We propose next to re-interpret activation parameters as pumping parameters. To this end, we point out two benchmark examples of amplitude equations that are known to involve pumping parameters. Our first example is the evolution equation for the laser intensity $I(t)$ that reads

$$\frac{d}{dt} I(t) = \lambda \, I(t) + \text{higher order terms} \tag{10}$$

The parameter λ reflects the impact of pumping processes versus processes that result in photon losses [26]. Our second example comes from population dynamics. The evolution equation for the size $n(t)$ of a population typically reads like [27]

$$\frac{d}{dt} n(t) = \lambda \, n(t) + \text{higher order terms} \tag{11}$$

In this context, the parameter λ reflects the difference between birth and death rate. In line with these two examples, we consider next physical self-organizing systems of the inanimate nature that satisfy the rescaled amplitude equations (6) and exhibit activation parameters that reflect pumping processes versus losses. In order to work out our main goal related to the issues pointed out in Table 1, we will assume that losses are negligible. In sum, for the activation parameters λ_k occurring in Eq. (6) we make the following association:

$$\lambda_k = \text{magnitude of pumping specific to mode} \quad k \tag{12}$$

2.3. Pumping, Entropy Production, and Rate of Entropy Production

Pumping is typically an irreversible process. This implies that the entropy S of the sub-system involved in the pumping process increases due to the irreversible pumping process: $d_{irr}\, S>0$. The increase of entropy due to an irreversible process, however, is known as entropy production. More precisely, the rate of entropy production r is defined by [28]

$$d_{irr} \; S = r \; dt \tag{13}$$

Irreversible pumping processes involve a positive rate of entropy production: $r>0$. It is plausible to assume that for a large class of pumping processes there exists a monotonically increasing

relationship between the magnitude of pumping λ and the rate of entropy production r. Accordingly, in these cases we have

$$r = \omega(\lambda) \tag{14}$$

with

$$\frac{d}{d\lambda}\omega(\lambda) \geq 0 \tag{15}$$

Let us exemplify Eqs. (14) and (15) by means of three examples.

In [29] a diffusion driven pumping processes has been discussed in detail. Particles representing local energy sources (energy depots) are diffusing through a one-dimensional channel from location A to location B. The channel has length L. The concentration of the particles is higher on the side A than on the side B of the channel. While diffusing through the channel each particle releases its energy and in doing so is pumping the system under consideration. For this pumping process it is assume that the magnitude of pumping is proportional to the particle current (or particle flux) J. We put

$$\lambda = \kappa J \tag{16}$$

where $\kappa>0$ is a constant factor. It can be shown [29] that J is given by

$$J = \frac{Q}{L}\Delta P \tag{17}$$

where $Q>0$ is the strength of the fluctuating force (roughly speaking: the diffusion constant) and $\Delta P=P(A)-P(B)$ is the difference in the particle probability density (roughly speaking: the density gradient) between the locations A and B. The rate of entropy production r is then related to λ by [29]

$$r = \frac{2Q^2}{L^2}\omega^*\left(\frac{L^2}{2Q\kappa}\lambda\right) \tag{18}$$

with

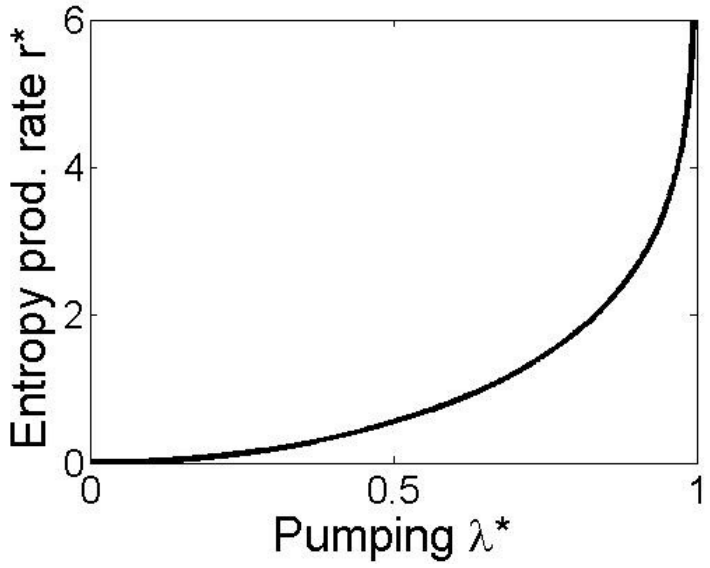
$$\omega^*(z) = z\log\left(\frac{1+z}{1-z}\right) \tag{19}$$

From Eqs. (18) and (19) it follows that r is a monotonically increasing function of λ, see Figure 2. That is,

$$\omega(\lambda) = \frac{2Q^2}{L^2}\omega^*\left(\frac{L^2}{2Q\kappa}\lambda\right) \tag{20}$$

satisfies the inequality (15) for any parameters L,Q, and κ. Note that the maximal pumping occurs in the limiting case $P(B)\to 0$. In this case, we have $P(A)=2/L$ and from Eqs. (16) and (17) we obtain $\lambda=2\kappa Q/L^2$. Since we have $\lambda=2\kappa Q/L^2$ we see that in this case the argument z in Eq. (19) approaches unity, i.e., the singularity point of the function ω^*. Re-evaluating the calculations in Ref [29], it can be shown that in the limiting case $P(B)\to 0$ we are dealing with an absorbing boundary $P(B)=0$ that requires a thermodynamic force that must become infinitely large. This infinitely large thermodynamic force is the reason why the rate of entropy production r goes to infinity, see Figure 2 again for $\lambda^*\to 1$.

Figure 2: Rate of entropy production versus pumping for pumping by means of a diffusion driven particle current. Rescaled variables are shown: $r^*=r\,L^2/(2Q^2)$ and $\lambda^*=\lambda\,L^2/(2Q\kappa)$. Graph is drawn from Eqs. (18) and (19).



In our second example, we assume that the multistable physical non-equilibrium system under consideration is pumped by means of an electric current I running through a wire of length L with Ohmic resistance R. The electric potential difference or voltage that drives the current is denoted by V. We assume that that Ohm's law holds: $I=V/R$. We can calculate the rate of entropy production r by studying first the local entropy production rate $\sigma(x)$ along the wire coordinate x, where r and σ are related to each other like [28]

$$r = \frac{d_{irr}\,S}{dt} = \int_0^L \sigma(x)dx \tag{21}$$

We have [28]

$$\sigma(x) = \frac{I\,E(x)}{T} \tag{22}$$

where $E(x)$ is the electric field and T denotes temperature. Substituting Eq. (22) into (21) and taking into account that the current I is constant and that

$$V = \int_0^L E(x)dx \tag{23}$$

we obtain

$$r = \frac{I\,V}{T} = \frac{R}{T}I^2 \tag{24}$$

In the final step in Eq. (24) we used Ohm's law. Next, we assume that the magnitude of pumping λ is proportional to the current I. Consequently, similar to Eq. (16), we put

$$\lambda = \kappa\,I \tag{25}$$

where $\kappa>0$ is a constant. Combining Eqs. (24) and (25) we obtain the final result

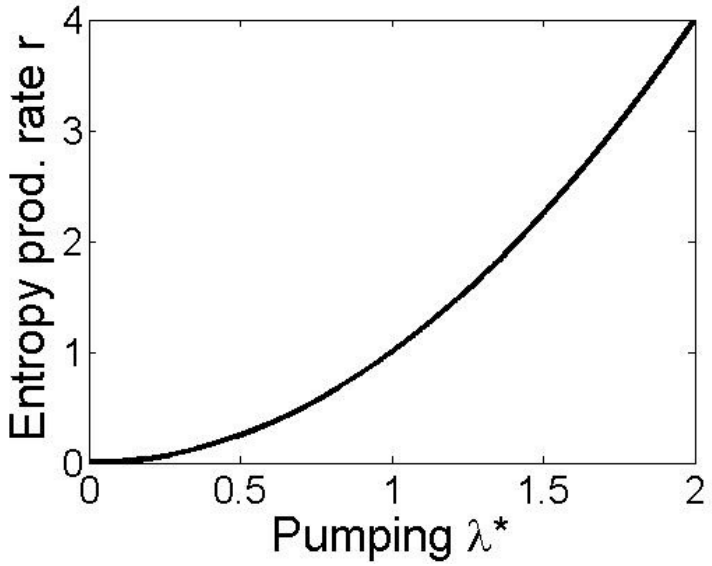
$$r = \frac{R}{T\kappa}\lambda^2 \tag{26}$$

That is, there is a quadratic relationship between rate of entropy production and pumping. In other words, when comparing Eqs. (14) and (26) we find that

$$\omega(\lambda) = \frac{R}{T\kappa}\lambda^2 \tag{27}$$

is a quadratic function that satisfies the inequality (15), see also Figure 3.

Figure 3: Rate of entropy production versus pumping for pumping by means of an electric current. Magnitude of pumping is shown in rescaled units: $\lambda^*=\lambda\sqrt{(R/T\kappa)}$. Graph is drawn from Eq. (27).



In our third example, we assume that the self-organized multistable physical system under consideration is pumped by means of a chemical reaction that involves n components (chemical substances). The rate of entropy production r can be computed from [28]

$$r = \frac{d_{irr}\ S}{dt} = \frac{V}{T} A\ v \tag{28}$$

where V is the volume and T the temperature of the sub-system in which the chemical pumping process takes place. The variable A denotes the affinity of the chemical reaction and v corresponds to the reaction velocity. We can compute the affinity from the molar Gibbs free energy $\Delta G<0$ of the chemical reaction like

$$A = -\Delta G + B(a_1,...,a_n) \tag{29}$$

The second term B depends on the activities a_k of the chemical substances $k=1,...,n$ (they frequently are related to the concentrations or partial pressures of the substances). In order to highlight the main point of our general argument (the monotonically increasing relationship between pumping and entropy production rate), we restrict ourselves to consider an irreversible chemical reaction (i.e. a reaction that exhibits only a forward reaction). In this case, the reaction velocity v is determine by the forward rate R_f of the reaction which in turn depends on the component activities a_k [28].

$$v = R_f(a_1,...,a_n) \tag{30}$$

In order to maintain a steady pumping process, we keep all activities a_k constant over time. This implies that the term B in Eq. (20) and the forward rate R_f in Eq. (30) become constants as well. Substituting Eqs. (20) and (30) into Eq. (28), we obtain

$$r = \frac{1}{T} V R_f \left(\left|\Delta G\right| + B\right) \tag{31}$$

The expression $v|\Delta G|$ (or $R_f\,|\Delta G|$) is a measure for the energy released per time unit due to the chemical reaction. We assume that the magnitude of pumping is proportional to that measure. Accordingly, we put

$$\lambda = \kappa R_f \left|\Delta G\right| \tag{32}$$

with $\kappa>0$ constant. Combining Eqs. (31) and (32), we obtain

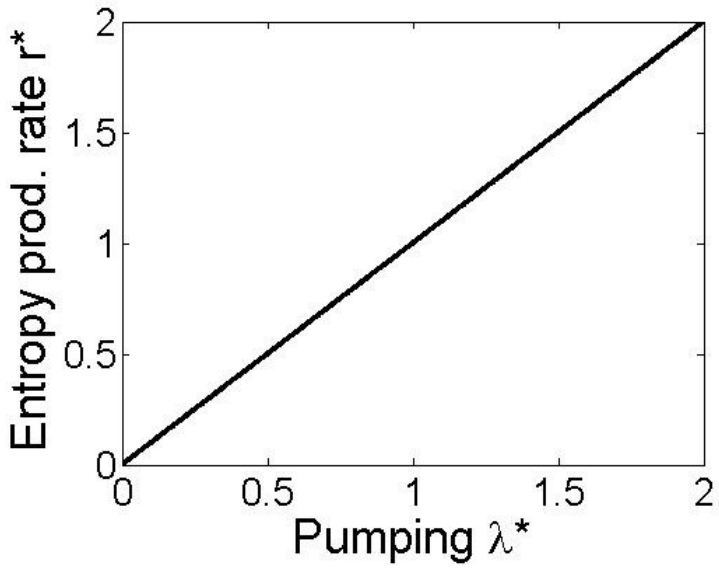
$$r = \frac{1}{T\kappa} V (\lambda + B^*) \tag{33}$$

with $B^*=R_f\,\kappa B$. In doing so, we have derived again a monotonically increasing relationship between pumping and rate of entropy production, namely, a linear one, see Figure 4. The omega-function (14) reads

$$\omega(\lambda) = \frac{1}{T\kappa} V (\lambda + B^*) \tag{34}$$

and clearly satisfies Eq. (15).

Figure 4: Rate of entropy production versus pumping for pumping by means of a forward chemical reaction. Magnitude of pumping and rate of entropy production are shown in shifted and rescaled units: $\lambda^*=\lambda+B^*$ and $r^*=r\,V/T\kappa$. Graph is drawn from Eq. (34).



2.4. Selection Principle for mode-mode Transitions: rate of Entropy Production

From the discussion in Sec. 2.1 it follows that mode-mode transitions occur when activation parameters decay below critical values (see Eq. (9)) such that the corresponding modes become unstable. At the bifurcation point a new mode emerges. From our stability analysis reviewed in Sec. 2.1., we conclude that the emerging mode must have an activation parameter that is larger than the critical threshold (see Eq. (8)) such that the emerging mode is stable. Let us denote the mode that the system exhibits before the bifurcation by pre-transition mode. Likewise, we refer to the emerging mode at the bifurcation point as post-transition mode. Let $\lambda_{k(pre)}$ and $\lambda_{k(post)}$ denote the activation parameters of pre-transition and post-transitions modes, respectively. From Eqs. (8) and (9) it follows that at the bifurcation point we have

$$\lambda_{k(pre)} < \frac{\lambda_{\max}}{g} < \lambda_{k(post)} \tag{35}$$

Since the omega-function (14) is a monotonically increasing function (see Eq. (15)), we can apply the function ω to each term in the inequality (35) and obtain

$$\omega\left(\lambda_{k(pre)}\right) < \omega\left(\frac{\lambda_{\max}}{g}\right) < \omega\left(\lambda_{k(post)}\right) \tag{36}$$

The function values in turn reflect the entropy production rates of the respective modes. Consequently, Eq. (36) can equivalently expressed in terms of

$$r_{k(pre)} < r_{crit} < r_{k(post)} \tag{37}$$

where r_{crit} denotes the critical rate of entropy production defined by $r_{\text{crit}}=\omega(\lambda_{\max}/g)$. Let Δr denote the difference between $r_{\text{k(pre)}}$ and $r_{\text{k(post)}}$ of the rate of entropy production rates prior and after the bifurcation: $\Delta r=r_{\text{k(post)}} - r_{\text{k(pre)}}$. Then from the inequalities (37) it follows that

$$\Delta r > 0 \tag{38}$$

In other words, Eq. (38) states that mode-mode transitions result in an increase of the entropy production rate. Vice versa, only mode-mode transitions are allowed that increase the rate of entropy production. Transitions of other kind are forbidden (selection principle). The selection principle defined by Eq. (28) is consistent with the selection principle proposed earlier by Swenson [30] and Swenson and Turvey [17]: the principle of maximum entropy production.

3. Application: Dynamic Message Buffer

We consider a buffer that can store a number of N messages. The buffer can take two actions: (i) send a "ready" signal in order to receive new messages and (ii) send out stored messages. Let w(t) denote the number of stored messages at time t. Then α(t)=w(t)/N is the relative used buffer space at time t and assumes values between 0 and 1. The parameter α will be considered as control parameter of our model. If the parameter α is close to zero the buffer needs to request new messages. In contrast, if α is close to 1, then the priority task of the buffer must be to send out stored messages. We use Haken's model (6) for two amplitudes in order to describe the dynamic behavior of the buffer. Accordingly, we have

$$\begin{aligned} \frac{d}{dt}\xi_1 &= \lambda_1(t)\,\xi_1 - g\xi_1\xi_2^2 - \xi_1^3 \\ \frac{d}{dt}\xi_2 &= \lambda_2(t)\,\xi_2 - g\xi_2\xi_1^2 - \xi_2^3 \end{aligned} \tag{39}$$

The two amplitudes reflect the activity of the two competing action modes: "send ready signal" (input mode) and "send message" (output mode). If ξ_1(t) > s ξ_2(t) with s>1 then the buffer sends the ready signal, i.e. it operates in the input mode. If ξ_2(t) > s ξ_1(t) then the buffer sends out stored messages, i.e., operates in the output mode. If none of the two inequalities are satisfied, then the buffer is undecided and takes no action. The parameter s makes sure that the buffer is only active when one of the two modes clearly dominates. There is a trade-off. The larger the parameter s is chosen, the more robust is the decision making in the sense that the selected mode must clearly dominate. However, the larger the parameter s is chosen, the larger is the potential domain in which the buffer is undecided. A large s is beneficial to the robustness of the decision process. In contrast, a parameter value s close to 1 is beneficial for making the undecided operation domain as small as possible.

Note that the activation parameters λ_1 and λ_2 depend only implicitly on time. In the first place, they depend on the control parameter $\alpha(t)$. If the parameter α is close to zero, then we need to activate

primarily the first (input) mode. If the parameter α is close to 1, then we need to activate primarily the second (output) mode. In order to satisfy these demands, we use

$$\lambda_1(t) = 1 - \alpha(t)$$
$$\lambda_2(t) = \alpha(t) \tag{40}$$

Note that if the relative used buffer space becomes 100 percent, then we have $\lambda_1 = 0$, which implies that the input mode becomes unstable [13]. In this case, the buffer exhibits the tendency to abandon the input mode. The dynamic model (39) and (40) for fixed (i.e. time-independent) parameter α was studied earlier [13] and it was shown that the model exhibits hysteresis. Consequently, there are two bifurcation points. If we increase gradually the parameter α from 0 to 1 then, the dynamic model switches from fixed points of the form $(\xi_1, \xi_2) = (>0,0)$ to fixed points $(\xi_1, \xi_2) = (0,>0)$ at [13]

$$\alpha_{c,2} = \frac{g}{1+g} \tag{41}$$

In our context, this is a switch from the input mode to the output mode. If we decrease the parameter α gradually from 1 to 0 then, the buffer dynamics switches from $(\xi_1, \xi_2) = (0,>0)$ to $(\xi_1, \xi_2) = (>0,0)$ at

$$\alpha_{c,1} = \frac{1}{1+g} \tag{42}$$

This corresponds to a switch from the output mode to the input mode. Note that $\alpha_{c,2} > \alpha_{c,1}$ because of g>1. While in the earlier study [13] the parameter α was externally manipulated by the experimenter, in our context, the buffer interacts with its environment and due to this interaction the control parameter α is changed. That is, if $\xi_1(t) > s\, \xi_2(t)$ then the ready signal is sent and messages are received such that α increases as a function of time. Likewise, if $\xi_2(t) > s\, \xi_1(t)$ then messages are sent out such that α decreases as a function of time. We assume that when the buffer is in the input mode then during each waiting period of $T_{in}>0$ time units there is a chance of $p_{in}>0$ that a message is received. Likewise, when the buffer is in the output mode then during each processing period of $T_{out}>0$ time units there is a chance of $p_{out}>0$ that a message successfully is sent out. If a message is received (a message is successfully sent out) then the relative used buffer space α is increased (decreased) by $1/N$: $\alpha \rightarrow \alpha + 1/N$ ($\alpha \rightarrow \alpha - 1/N$). In sum, the dynamic buffer and its interactions with the environment are described by Eqs. (39) and (40) and by the stochastic buffer-environment interactions just described.

We solved Eqs. (39) and (40) numerically using an Euler forward scheme with single time step τ. The simulation parameters were: $g=2$, $\tau=0.01$ time units [TU], $s=1.1$, $T_{in}=T_{in}=1$ [TU], $p_{in}=0.5$, $p_{in}=0.8$, $N=100$. Initial values were $\xi_1(t=0)=0.1$ and $\xi_2(t=0) = 0.01$. Figure 5 shows the evolution of the relative used buffer size α. Figure 6 depicts the amplitudes $\xi_1(t)$ (solid line) and $\xi_2(t)$ (dashed line) as functions of time. After a transient period, the dynamic buffer exhibits an oscillatory behavior. When α approaches the upper critical value $\alpha_{c,2} = 2/3$, then a bifurcation from the input to the output mode occurs. The buffer goes into the output mode and sends out messages. The relative used buffer spaces α decreases. When the relative used buffer space α approaches the lower critical value $\alpha_{c,1} = 1/3$, then a bifurcation from the output to the input mode occurs. The buffer switches into the input mode and sends the ready signal. The buffer receives (at random intervals) new messages and the relative used buffer size α increases. The messages received and sent out are illustrated in Figure 7.

Figure 5: Relative used buffer size α as a function of time t. During a transient period, the control parameter α increases. Subsequently, α oscillates between the two critical boundaries described by Eqs. (41) and (42). For g=2 we have that $\alpha_{c,1}$ = 1/3 and $\alpha_{c,2}$ = 2/3. The relative used buffer size α increases (decreases) when $\xi_1(t) > s\,\xi_2(t)$ ($\xi_2(t) > s\,\xi_1(t)$), cf. with Figure 6.

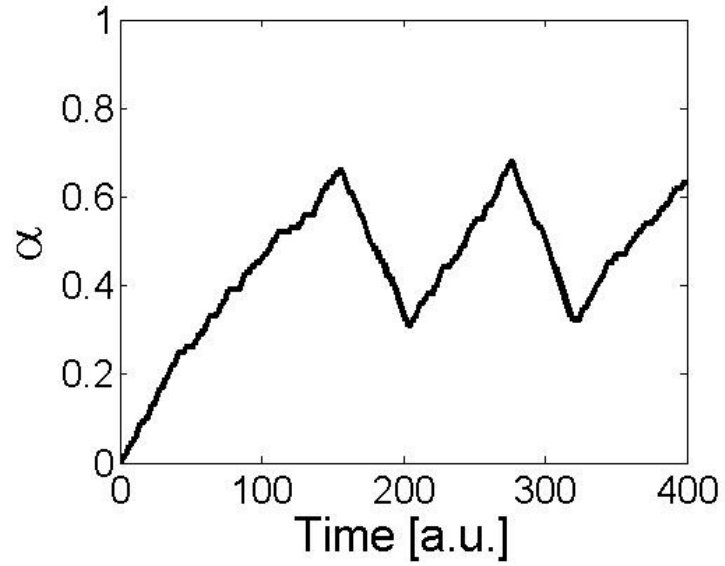


Figure 6: Amplitudes $\xi_1(t)$ (solid line) and $\xi_2(t)$ (dashed line) as functions of time as computed for the dynamic message buffer model described in Sec. 3. When α approaches the upper critical value $\alpha_{c,2}$ = 2/3 a bifurcation from the input to the output mode occurs. Likewise, when α approaches the lower critical value $\alpha_{c,1}$ = 1/3 a bifurcation from the output to the input mode occurs, cf. Figure 5.

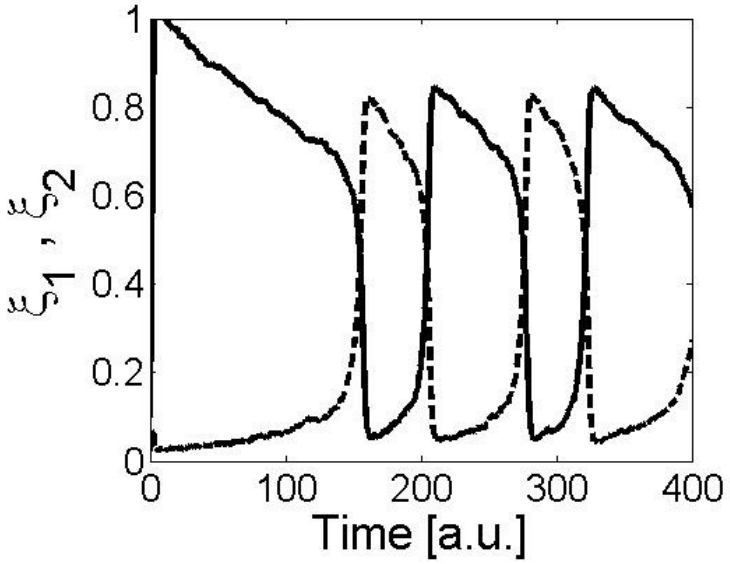
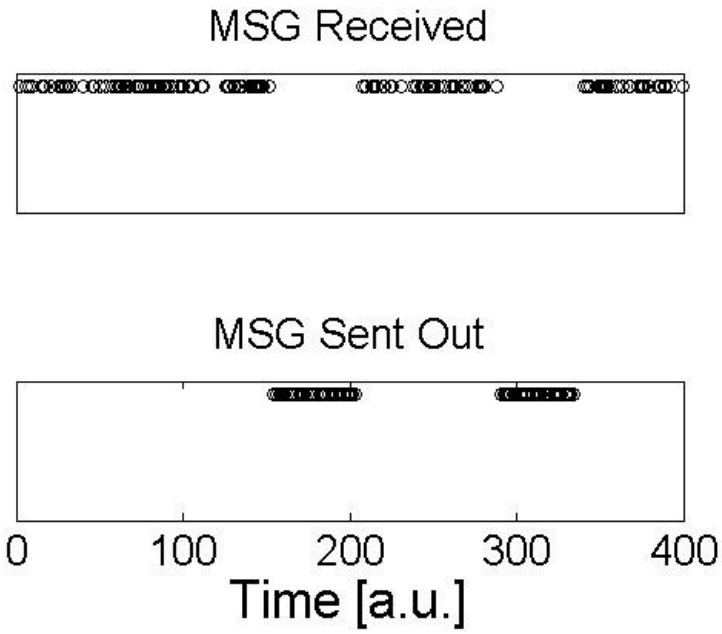


Figure 7*:* Messages received during periods in which the buffer operates in the input mode, i.e., when $\xi_1(t) > s\ \xi_2(t)$ holds (top panel). Messages sent out during periods in which the buffer operates in the output mode, i.e., when $\xi_2(t) > s\ \xi_1(t)$ holds (bottom). Each circle corresponds to one message.



We also determined the activation parameters λ_1 and λ_2 as functions of time. Figure 8 shows the simulation results. In order to demonstrate that the buffer satisfies the thermodynamic selection principle defined by the inequality (38), we assumed a linear or quadratic relationship between activation parameters λ_k and the rate of entropy production. The linear relationship may reflect a chemical pumping mechanism as discussed in Sec. 2.3 (see also Figure 3), whereas the quadratic relationship may reflect the electronic pumping addressed again in Sec. 2.3 (see also Figure 4). Figures 9 and 10 depict the rate of entropy production of the active mode as a function of time for the two pumping mechanisms. To this end, we determined at every time point the active mode and then calculated the rate of entropy production from the activation parameter λ_k of that mode. More precisely, for the linear case we used

$$r(t) = c_1 \lambda_k\ (t)\ + c_2 \tag{43}$$

where the index k denote the active mode at time point t. For sake of simplicity, we used c_1=1 and c_2=0. Likewise, for the quadratic case, we used

$$r(t) = c_1\ [\lambda_k\ (t)]^2 + c_2 \tag{44}$$

again with c_1=1 and c_2=0. Figures 9 and 10 illustrate the thermodynamic selection principle: at mode-mode transitions (input-to-output transitions or output-to-input transitions) the rate of entropy production increases. The jumps in the graphs shown in Figures 9 and 10 satisfy Δr>0, that is, the inequality (38) derived in Sec. 2.4.

Figure 8: Activation parameters $\lambda_1(t)$ (solid line) and $\lambda_2(t)$ (dashed line) as functions of time as computed from Eq. (40) and the trajectory $\alpha(t)$ shown in Figure 5.

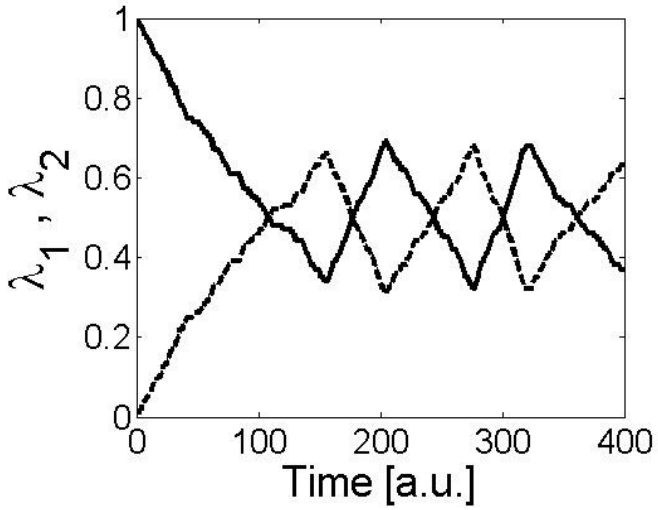


Figure 9: Rate or entropy production of the active mode computed from activation parameters $\lambda_1(t)$ and $\lambda_2(t)$ shown in Figure 7. Entropy production was assumed to be a linear mapping of λ_k, see Eq. (43).

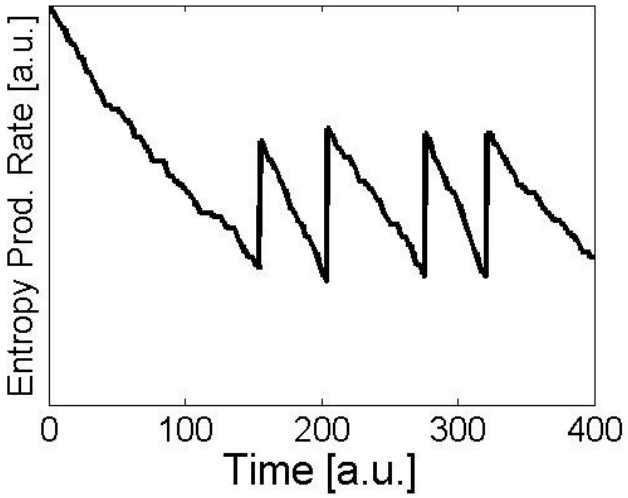
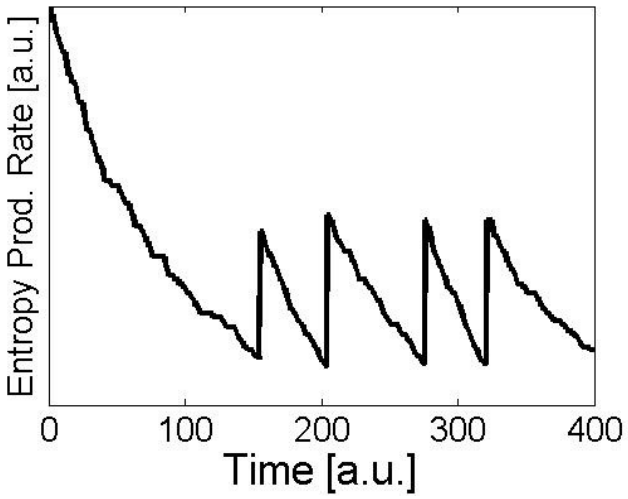


Figure 10*:* Rate or entropy production of the active mode computed from activation parameters $\lambda_1(t)$ and $\lambda_2(t)$ shown in Figure 7. Entropy production was assumed to be a quadratic mapping of λ_k, see Eq. (44).



4. Conclusions

There were two main goals of our study. First, we pointed out that physical, non-algorithmic systems may be used to solve problems in artificial intelligence. Second, we demonstrated that mode-mode transitions in multistable systems may satisfy a selection principle that is of thermodynamic nature: the increase of the rate of entropy production. To this end, we considered a generic model for pattern formatting systems: the amplitude equations of Haken's pattern recognition algorithm. They do not only reflect the amplitude dynamics of pattern formatting physical systems such as lasers and convection cells, they also can be used to construct intelligent algorithm that solve various perceptual, behavioral and cognitive tasks [2,5,6,7,8,13,15] and solve problems in the field of artificial intelligence in general. For example, in Sec. 3 we used this model to construct a dynamic message buffer.

A striking feature of the multistable pattern formatting system is that mode-mode transitions satisfy a simply rule: transitions occur from modes with smaller activation parameters towards modes with larger activation parameters. That is, at a bifurcation point the activation parameter (feedback parameter) of the active mode increases. Mathematically speaking, let $\lambda_{k(pre)}$ and $\lambda_{k(post)}$ the feedback parameters of the "disappearing" and emerging modes at the bifurcation point. Then we have $\Delta\lambda=\lambda_{k(post)} - \lambda_{k(pre)}>0$. Bifurcations that would involve a decrease of the activation parameter are forbidden because they violate the inequality $\Delta\lambda>0$ (selection principle). In Sections 2.2, 2.3, and 2.4 we argued that activation parameters can be regarded as measures for entropy production rates. In particular, for three examples we derived the mappings between the entropy production rates r and the activation parameters or pumping parameters λ. In all three examples, the mappings were found to be monotonically increasing functions. With such monotonically increasing mappings at hand, the aforementioned selection principle can be translated from the field of dynamical systems theory into the field of thermodynamics. Accordingly, the inequality

$$\Delta\lambda > 0 \tag{45}$$

(dynamic systems theory) is translated into the inequality $\Delta r>0$ (thermodynamics), see Eq. (38).

Let us reiterate the meaning of this key result: the inequality $\Delta r>0$ states that mode-mode transitions are forbidden that involve a decreases of the rate of entropy production of the active mode. Mode-mode transitions involve an increase of the rate of entropy production associated with the active mode.

Acknowledgement

The author gratefully acknowledges the support for this work by Defense Advanced Research Projects Agency (DARPA) Physical Intelligence (subcontract HRL 000708-DS). The views, opinions, and/or findings contained in this article are those of the author and should not be interpreted as representing the official views or policies, either expressed or implied, of the DARPA or the Department of Defense.

References

[1] Haken, H. (1988). "Nonequilibrium phase transitions in pattern recognition and associate memory", *Zeitschrift fur Physik B*, 70, pp. 121-123

[2] Haken, H. (1991). "Synergetic computers and cognition", Springer, Berlin

[3] Bestehorn, M., Haken, H. (1991). "Associative memory of a dynamical system: an example of the convection instability", *Zeitschrift fur Physik B*, 82, pp. 305-308

[4] Bestehorn, M., Friedrich, R. (1999). "Rotationally invariant order parameter equations for natural patterns in nonequilibrium systems", *Physical Review E*, 59, pp. 2642-2652

[5] Fuchs, A., Haken, H. (1988). "Pattern recognition and associative memory as dynamical process in a synergetic system", *Biological Cybernetics*, 60, pp. 17-22

[6] Ditzinger, T., Tuller, B., Kelso, J.A.S. (1987). "Temporal patterning in an auditory illusion: the verbal transformation effect", *Biological Cybernetics*, 77, pp. 23-30

[7] Ditzinger, T., Haken, H. (1989). "Oscillations in the perception of ambigious patterns: a model based on synergetics", *Biological Cybernetics*, 61, pp. 279-287

[8] Daffertshofer, A., Haken, H. (1994). "A new approach to recognition of deformed patterns", *Pattern recognition*, 27, pp. 1697-1705

[9] Yudashkin, A. A. (1996). "Bifurcations of steady-state solutions in the synergetic neural network and control of pattern recognition", *Auto Remote Control*, 57, pp. 1647-1653

[10] Bresslof, P. C., Roper, P. (1998). "Stochastic dynamics of the diffusive Haken model with subthreshold periodic forcing", *Physical Review E*, 58, pp. 2282-2287

[11] Haken, H., Schanz, M., Starke, J. (1999). "Treatment of combinatorial optimization problems using selection equations with cost terms", *Physica D*, 134, pp. 227-241

[12] Starke, J., Kaga, T., Schanz, M., Fukuda, T. (2005).). "Experimental study on self-organized and error resistant control of distributed autonomous robotic systems", *International Journal of Robotics Research*, 24, pp. 465-486

[13] Frank, T.D., Richardson, M. J., Lopresti-Goodman, S. M., Turvey, M. T. (2009). "Order parameter dynamics of body-scaled hysteresis and mode transitions in grasping behavior", *Journal of Biological Physics*, 35, pp. 127-147

[14] Frank, T.D., van der Kamp, J., Savelsbergh, G. J. P. (2010). "On a multistable dynamic model of behavioral and perceptual infant development", *Developmental Psychobiology*, 52, pp. 352-371

[15] Frank, T.D. (2009). "On a multistable competitive network model in the case of an inhomogeneous growth rate spectrum with an application to priming", *Physics Letters A*, 373, pp. 4127-4133

[16] Frank, T.D. (2011). "Multistable selection equations of pattern formation type in the case of inhomogeneous growth rates: with applications to two-dimensional assignment problems", *Physics Letters A*, 375, pp. 1465-1469

[17] Swenson, R., Turvey, M. T. (1991). "Thermodynamic reasons for perception-action cycles", *Ecological psychology*, 3, pp. 317-348

[18] Frank, T.D., Sondermann, M., Ackemann, T., Friedrich, R. (2005). „Parametric data analysis of bistable stochastic systems", *Nonlinear Phenomena in Complex Systems*, 8, pp. 193-199

[19] Chiangga, S., Frank, T.D. (2010). "Stochastic properties of single-transverse-mode vertical-cavity surface-emitting lasers", *Nonlinear Phenomena in Complex Systems*, 13, pp. 32-37

[20] Bestehorn, M., Friedrich, R., Haken, H. (1989). "Two-dimensional traveling wave patterns in nonequilibrium systems", *Zeitschrift fur Physik B*, 75, pp. 265-274

[21] Bödeker, H.U., Frank, T.D., Friedrich, R., Purwins, H.G. (2008). „Stochastic dynamics of dissipative solitons in gas-discharge systems", in Riccardi and Roman (Eds) *Amomalous Fluctuation Phenomena in Complex System: Plasmas, Fluids, and Financial Models*, Research Signpost, Kerala, pp.145-184

[22] Bödeker, H.U., Röttger, M.C., Frank, T.D., Friedrich, R., Purwins, H.G. (2003). „Noise-covered drift bifurcation of dissipative solitons in a planar gas-discharge system", *Physical Review E*, 67, pp 056220

[23] Bödeker, H.U., Liehr, A.W., Röttger, M.C., Frank, T.D., Friedrich, R., Purwins, H.G. (2004). "Measuring the interaction law of dissipative solitons", *New Journal of Physics*, 6, pp. 61.1-62.18

[24] Liehr, A.W., Bödeker, H.U., Röttger, M.C., Frank, T.D., Friedrich, R., Purwins, H.G. (2003). "Drift-bifurcation detection for dissipative solitons", *New Journal of Physics*, 5, pp. 89.1-89.9

[25] Markevich, N. I., Hoek, J. B., Kholodenko, B. N. (2004). "Signaling switches and bistability arising from multisite phosphorylation in protein kinase cascades", *Journal of Cell Biology*, 164, pp. 353-359

[26] Haken, H. (1991). "Light – Laser Light Dynamics", North Holland, Amsterdam

[27] Goel, N. S., Miatra, S. C., Montroll, E. W. (1971). "On the Volterra and other nonlinear models of interacting populations", *Review of Modern Physics*, 43, pp. 231-276

[28] Kondepudi, D., Prigogine, I. (1998).). "Modern thermodynamis", John Wiley and Sons, New York

[29] Frank, T. D. (2010). "Pumping and entropy production in non-equilibrium drift-diffusion systems: a canonical-dissipative approach", *European Journal of Scientific Research*, 46, pp. 136-146

[30] Swenson, R. (1989). "Emergent attractors and the law of maximum entropy production: foundations to a theory of general evolution", *Systems Research*, 6, pp. 187-197.